Phase properties of reflected light in photonic band gap

Qiao-Feng Dai,[1,a)] Sheng Lan,[1] Li-Jun Wu,[1] and He-Zhou Wang[2]
[1]*Laboratory of Photonic Information Technology, School for Information and Optoelectronic Science and Engineering, South China Normal University, Guangzhou 510006, China*
[2]*State Key Laboratory of Optoelectronic Materials and Technologies, Zhongshan (Sun Yat-Sen) University, Guangzhou 510275, China*

(Received 30 October 2009; accepted 10 March 2010; published online 7 May 2010)

We find that the phase shifts of reflected light within band gap of two-dimensional photonic crystal (PC) are as follows: with frequency altering from the lower edge to the upper edge of first stop band, the reflection phase shift varies from $-\pi$ to 0 for the PC's unit cell with the high-index material near the center, while it varies from 0 to π for that with low-index material near the center. For the higher-order stop band, there exists a certain value of filling fraction, which makes the phase shifts in higher-order stop bands almost the same as that in the first stop band. When the filling fraction is far from that value, the phase shifts are significantly different. The further study on the Bloch modes demonstrates that their distribution of electric field and magnetic field determines the phase shifts. Moreover, we have found that, in the overlap area of transverse magnetic and transverse electric stop band, the phase difference between two polarizations of reflected light can remain invariant in a broad frequency region. Based on this property, the broadband and angle-insensitive phase retarders are designed. These interesting phase characteristics will bring about many potential applications. © *2010 American Institute of Physics*. [doi:10.1063/1.3383045]

I. INTRODUCTION

Photonic crystals (PCs) are artificial structures consisting of periodic arrays of dielectric or metal materials.[1,2] The unique properties of PC have been extensively explored.

Amplitude, frequency, and phase are three important parameters indicating the characteristics of light. So far, most investigations of PC have been made on the amplitude and frequency of transmitted and reflected light. By comparison, investigations on the phase properties are relatively fewer.

In the PC pass band, a single wavelength wave plate utilizing the transmission phase shift has been theoretically proposed[3] and experimentally investigated in the microwave region.[4,5] The two-dimensional (2D) metal PC has also demonstrated its ability to change the polarization of transmitted light in the experiment.[6] A kind of metamaterials wave plate is substantiated in realists simulation,[7] and another PC wave plate is proposed based on self-collimation.[8]

The most crucial properties and applications of PC appear in the photonic band gap.[9–11] Recently, a few researchers reported that in the case of normal incidence, the reflection phase shift amounts to π from one band edge to another in the first stop band.[12,13] We proposed a method to design broadband half-wave plate in stop band of PC.[14] However, a great number of phase characteristics in the PC band gap have not yet been revealed. In this paper, we show the reflection phase properties and relationship among different stop bands of 2D PC, and give explanations to the rules of the phase shift. It is found that the refraction index distribution and filling fraction in unit cell play an important role in the reflection phase shift in stop band. Furthermore, based on the relationship between the phases of transverse electric (TE) and transverse magnetic (TM) reflected light, we expand the method[14] to design broadband and angle-insensitive phase retarders with arbitrary phase shift difference.

This paper is arranged as follows. In Sec. II, the theory of calculating the reflection phase is introduced. In Sec. III, we investigate the influence of refraction index distribution on the reflection phase in first stop band. In Sec. IV, we investigate the influence of filling fraction on the reflection phase in higher-order stop band. In Sec. V, the dependence of reflection phase on incident angle is researched. In Sec. VI, the relationship between two polarizations is discussed. In Sec. VII, broadband and angle-insensitive phase retarders are designed and discussed. Finally we briefly summarize the paper in Sec. VIII.

II. THEORY

The 2D transfer matrix method (TMM) (Ref. 15) is adopted to calculate complex reflection coefficient and obtain reflection phase shift. On one hand, TMM is very effective for calculation of complex reflection coefficient. On the other hand, there is more freedom to set unit cell structure in TMM, which allows us to adjust structural parameters in a broad region to optimize structures. A complex reflection coefficient is defined as $r=u_r/u_{\text{in}}$, where u_{in} is the field of incident light, and u_r is the field of the reflected light. The zeroth order reflection coefficient is obtained as[15]

$$r^{(0)} = \frac{u_r^{(0)}}{u_{\text{in}}^{(0)}} = |r^{(0)}|e^{i\varphi}, \tag{1}$$

where $|r^{(0)}|$ is the zeroth order reflection coefficient and φ is the phase shift in the reflected light. By calculating the phase shifts in reflected light with different polarizations, we are able to figure out the polarization change in reflected light relative to the incident light. Any incident wave can always be decomposed to TE and TM wave with certain phase dif-

a)Author to whom correspondence should be addressed. Electronic mail: daiqf@scnu.edu.cn.

ference (e.g., phase difference of zero for linear polarization). Therefore, the polarization of reflected light can be obtained by comparing the phase shift in the reflected TE and TM field.

III. THE PHASE PROPERTIES OF SINGLE POLARIZATION REFLECTED LIGHT IN THE FIRST STOP BAND

For TM wave (i.e., the electric field vector is parallel to the cylinders), when the material with high index of refraction is near the center of the unit cell, the reflection phase shift varies from $-\pi$ at one band edge to zero at another band edge of the first stop band. When low index material is near the center, the reflection phase shift varies from zero at one band edge to π at another band edge of the first stop band. The explanation for this phenomenon is that, in the first stop band, the electric field of the lower band edge is mainly distributed in the high index material of the unit cell, while the case is the opposite for electric field at the upper band edge.

First, a 2D square lattice consisting of dielectric rods with a background of air is considered. The index of refraction of the rods is 3.4, and the rod radius is $r=0.4a$, where a is the lattice constant. The length along the z direction is $64a$ [Fig. 1(e)]. The direction of the light incident from the air is along Γ-X (shown as the z direction in the figure), normal to the surface of the PC. Using TMM, the dependence of the reflectance and reflection phase shift on frequency is plotted, as shown in Figs. 1(a) and 1(b), respectively. In Fig. 1(b), the reflection phase shift at the lower edge A of the first stop band is approximately -0.972π, close to $-\pi$, while the shift at the upper band edge is approximately -0.018π, close to zero. Then 2D square lattice consisting of air rods in dielectric background is considered. The index of refraction of the dielectric material is 3.4, the air rod radius $r=0.4a$, and the length in the z direction is $64a$ [Fig. 1(e)]. The direction of light incident from the dielectric material is also along Γ-X, normal to the surface of the PC. Using TMM, the dependence of the reflectance and reflection phase shift on frequency is plotted, as shown in Figs. 1(c) and 1(d), respectively. In Fig. 1(d), the phase shift at the lower band edge B of the first stop band is about 0.012π, close to zero, while the shift at the upper band edge is 1.073π [equivalently shown as -0.927π in Fig. 1(d)], close to π.

The phase shift at the stop band edge can be explained by the Bloch mode of the PC band edge.[13] Using MIT PHOTONIC BAND package,[16] we obtain the electromagnetic field Bloch modes at the lower band edge A and B of the first stop band in two types of PC, as shown in Fig. 1(e). The figure shows 3×3 cells. The dashed line corresponds to the unit cell edge where the light is incident. At the lower edge A of the first stop band of dielectric rods structure, the electric field mainly concentrates near the high index material in the center of the unit cell. E_y near the edge of the unit cell is about zero, while H_x has a relatively large value. In order to meet the continuous boundary condition at the edge of the crystal, the superposition of the electric fields of incident light and reflected light should result in a cancellation of both fields. Correspondingly, the superposition of the magnetic fields should lead to an intensification of both fields. Therefore, the phase shift should be $\pm\pi$. In such a frequency, the reflection of PC is analogous with that of perfect electric conductance. On the contrary, at the lower band edge B of the first stop band in the air rod structure, the electric field mainly concentrates near the high index material around the unit cell. E_y near the edge of the unit cell has a relatively large value, while H_x is approximately zero. In order to meet the continuous boundary condition in the boundary of the crystal, the superposition of the magnetic fields of the incident light and reflected light should result in the cancellation of the both fields. Correspondingly, the superposition of the electric field should result in the intensification of the both fields. Therefore, the reflection phase shift should be zero. In this frequency, the reflection of PC is similar to that of a perfect magnetic conductance.

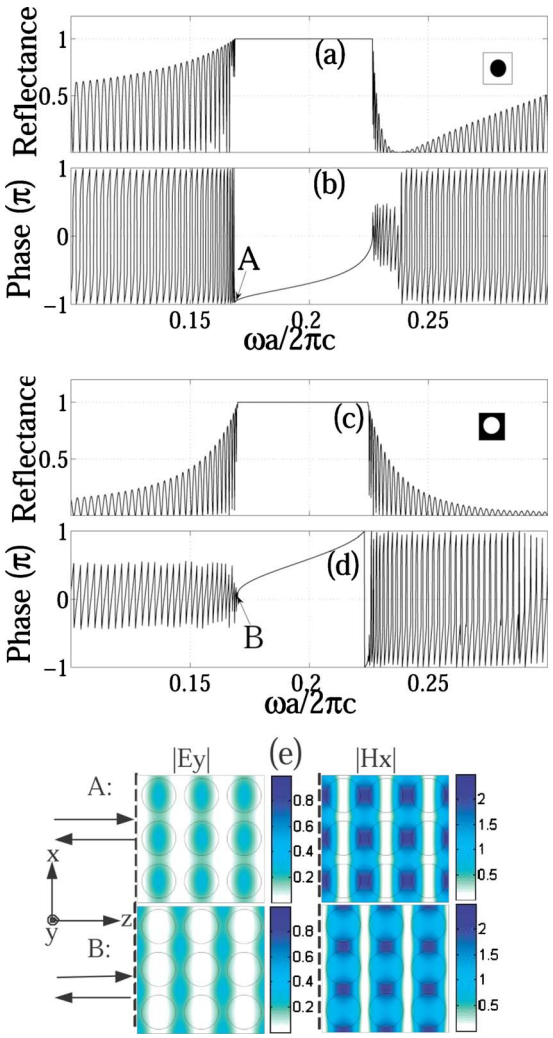

FIG. 1. (Color online) (a) and (b) show the dependence of TM polarized reflectance and reflection phase shift on frequency, respectively, in the PC with dielectric rods in an air background; (c) and (d) show the dependence of TM polarized reflectance and reflection phase shift on frequency, respectively, in the PC with air rods in a dielectric background. The dielectric index of refraction is $n=3.4$, $L=64a$, and $r=0.4a$. Points A and B are the lower edge of the first stop band in (b) and (d), respectively. (e) shows the electromagnetic field Bloch modes at point A and B in 3×3 unit cells. The dashed lines on the left side of the cells denote the reflection interface.

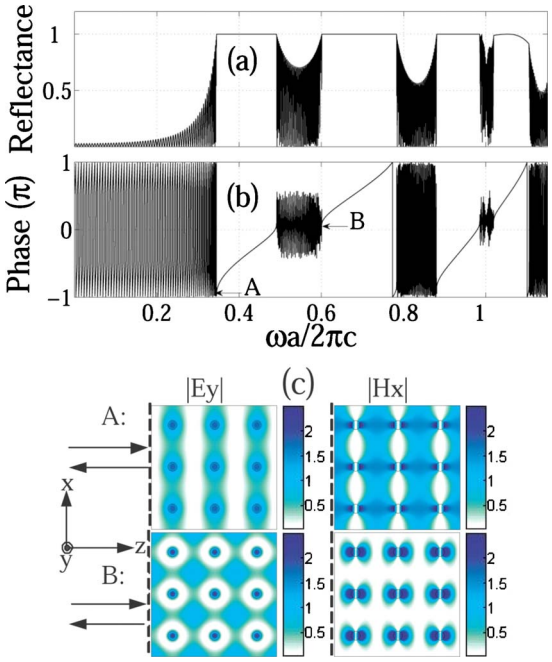

FIG. 2. (Color online) (a) and (b) show the dependence of TM polarized reflectance and reflection phase shift on frequency, respectively, in the PC with dielectric rods in an air background. The dielectric index of refraction $n=3.4$, $L=64a$, and $r=0.11a$. Point A and B are the lower edges of the first and second stop bands, respectively. (c) shows the electromagnetic field Bloch modes at point A and B in 3×3 unit cells. The dashed lines on the left side of the cells denote the reflection interface.

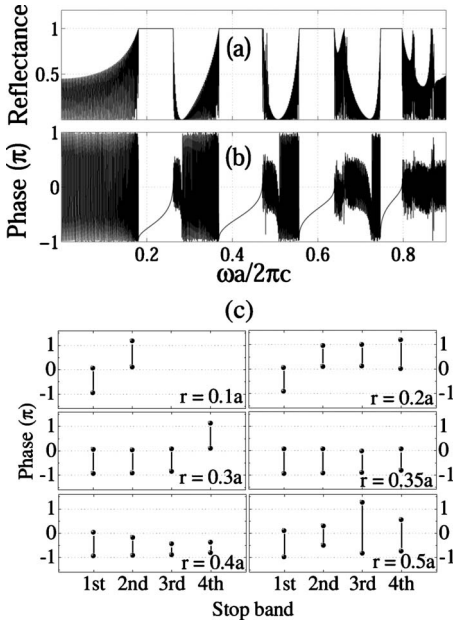

FIG. 3. (a) and (b) show the dependence of TM polarized reflectance and reflection phase shift on frequency, respectively, in the PC with dielectric rods in an air background. The dielectric index of refraction $n=3.4$, $L=64a$, and $r=0.35a$. (c) shows the phase regions of different order stop band with different rod radii, where the phase regions are denoted by two points linked by line. The two points indicate the upper and lower edges of each stop band.

IV. THE PROPERTIES OF SINGLE POLARIZATION REFLECTED LIGHT IN THE HIGHER-ORDER STOP BAND

In most cases, the reflection phase shift in the higher-order stop band differs from that of the first stop band. In general, the stop bands are found to appear between the dielectric bands and air bands, and this can be theoretically deduced by variational theorem.[17] For the lower-order stop band, such phenomena are obvious owning to the relatively simple band structure. However, it comes to be complicated for the higher-order stop bands. Besides between the dielectric bands and air bands, the higher-order stop bands can also appear between two dielectric bands, in which Mie resonance plays an important role.[18] For the various formation mechanisms of higher-order stop band, electric field does not necessarily concentrate near the high index of refraction material in the unit cell at the lower edge, and it does not necessarily concentrate near the low index of refraction material in the unit cell at the upper edge.

The dielectric rod radius of the 2D square lattice are changed to $r=0.11a$, where a is the lattice constant, and the length in the z direction is $64a$ [Fig. 2(c)]. The direction of light incident from the air is along Γ-X (shown as the z direction in the figure), normal to the surface of PC. The reflection of TM wave and the dependence of the reflection phase shift on frequency are plotted in Figs. 2(a) and 2(b), respectively. As can be seen from Fig. 2(b), the lower edge A of the first stop band approximates to $-\pi$, while its upper band edge approximates to zero. The lower edge B of the second stop band approximates to zero while its upper band edge approximates to π. In Fig. 2(c), we have plotted the Bloch mode of the electromagnetic fields at the lower edges A and B of the two stop bands, respectively. At point A, since the electric field on the boundary of the unit cell is to zero, the reflection phase shift should be close to $-\pi$. At point B, since the magnetic field on the boundary of the unit cell is zero, the reflection phase shift should be close to zero. Note that at the lower edge A of the first stop band, the electric field concentrates near the high refractive index material in the unit cell, while at the lower edge B of the second stop band, the electric field near the boundary of the unit cell has a large value instead of zero, despite that the high index of refraction material in the center of the unit cell is distributed with high intensity electric field.

When the filling fraction changes, the amount of difference between the reflection phase shift in the higher-order stop band and that in the first stop band varies correspondingly. To certain index of dielectric rods, there exists a corresponding value of filling fraction that enable the reflection phase shift near the lower or upper edge of higher-order stop band has a slight difference from $-\pi$ or zero. Filling fraction that is larger or smaller than this value will lead to a larger difference of reflection phase shift at the edge of higher-order stop band.

The refraction index of dielectric rods is fixed to 3.4. We obtain different reflection phase shift by gradually enlarging the rod radius. It is found that a radius of $0.35a$ results in the smallest difference of reflection phase shift near the edge of higher-order stop band, as is shown in Fig. 3. Figure 3(a) shows the dependence of TM wave reflection on frequency, and Fig. 3(b) shows the dependence of TM reflection phase shift on frequency. Compared with Fig. 2(b), there is a sig-

nificant decline in the phase shift in the second and the fourth stop band in Fig. 3(b). The reflection phase shifts at the lower and upper edge of the second and fourth stop band approach $-\pi$ and zero, respectively. When r is larger or smaller than this value, the reflection phase shift at the higher-order stop band edge is similar to that in Fig. 2(b). In other words, the reflection phase shift at the higher-order stop band edge differs greatly from that at the first stop band edge. In order to show the difference clearly, the phase regions corresponding to each stop band are presented in Fig. 3(c) with different rod radii (or with different filling fractions). Here, the normalized frequencies investigated are limited to be less than 0.9. As can be seen from the Fig. 3(c), the phase regions of first stop bands are all near to $(-\pi,0)$ for different rod radius, and the phase regions of higher-order stop bands are near to that of first stop band only for rod radius of $0.35a$. This is very interesting, and an analog with one-dimensional (1D) PC is given to explain the phenomenon. In an ideal 1D quarter-wave stack with equal optical path lengths in each material, the reflection phase shift at the higher-order stop band is the same as that at the first stop band. When optical path lengths in each material are changed, the reflection phase shift at the higher-order stop band edge will gradually move away from that at the first stop band edge. The 2D PC with dielectric rods in the air behaves like a dielectric stack with thick high index layers separated by thin air layers. A change in the filling fraction of high index rods equals to a change in the effective optical path in the high index dielectric layer. For an index of 3.4 in dielectric rods, it is found that a radius of $0.35a$ results in an equivalence in effective optical path of high index dielectric layer and air layer, as well as small reflection phase shift differences at the corresponding high and low stop band edge. As the radius increases or decreases, the effective optical paths in the high and low index layers are no longer equal, and the difference between the reflection phase shifts at the corresponding high and low stop band edge increases.

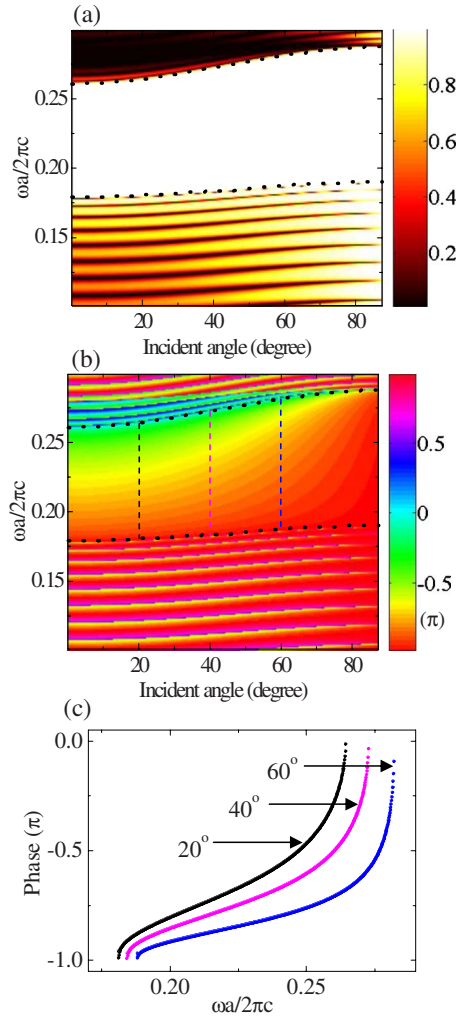

FIG. 4. (Color online) (a) shows the reflectance as a function of normalized frequency and incident angle and (b) shows the corresponding reflection phase as a function of normalized frequency and incident angle. The band edges are marked with dotted lines. The three dashed lines in (b) denote frequency domain of stop band for the incident angle of 20°, 40°, and 60°, respectively. (c) shows the reflection phase as a function of normalized frequency for the incident angle of 20°, 40°, and 60° in stop band.

V. THE REFLECTION PHASE FOR DIFFERENT INCIDENT ANGLE

The properties of reflection phase for different incident angle have also been investigated. It is found that the variation behavior of phase shift in stop band is not sensitive to incident angle generally. The 2D square lattice consisting of dielectric rod with radius of $0.35a$ is considered as a sample for TM wave. The reflectance as a function of normalized frequency and incident angle is shown with quasi-three-dimensional image in Fig. 4(a), and corresponding reflection phase as a function of normalized frequency and incident angle is shown with quasi-three-dimensional image in Fig. 4(b). The stop band edges are marked with dotted lines. In Fig. 4(b), the phase shift at lower (or upper) edge of stop band is near to $-\pi$ (or zero) even for bigger incident angle, and the variation behaviors of phase in whole stop band have similar fashion for different incident angle. The slight difference lies in: for smaller incident angle, the phases increase evenly in whole stop band with increasing normalized frequency; for bigger incident angle, they increase gently at first, then drastically with increasing normalized frequency. In order to show them more directly, the reflection phases in stop band for incident angle of 20°, 40°, and 60° are presented in Fig. 4(c), respectively. The corresponding frequency domains are marked with dashed lines in Fig. 4(b). In Fig. 4(c), the similar variation behaviors of phase are clearly showed for different incident angle. This property would be useful to design application devices based on reflection phase on 2D PC.

VI. THE REFLECTION PHASE RELATIONSHIP BETWEEN TWO POLARIZATIONS

Although phases in different stop bands are different, the phases in all stop bands change smoothly with frequency, while they change dramatically with frequency in the pass bands. For TE wave, phase change is similar to that of TM wave. In the common high reflection region, the phases of the two polarizations change smoothly with frequency. With this property, wave plates can be obtained. To certain inci-

dent direction, it is not difficult to realize a broad common reflection region for TE and TM wave. In the common reflection region, the relative position of stop bands can be varied by adjusting structural parameters, and consequently, the phase shift difference between TE and TM waves can be adjusted to a set value, say, π or $\pi \pm \pi/2$, corresponding to half-wave plate and quarter-wave plate, respectively. More importantly, since the phase shift changes smoothly inside the stop band, the reflection phase difference can remain constant in a broad frequency range, and broadband phase retarder can be realized.

VII. APPLICATION

Waveguide and microcavity are two important applications for PC. Optical waveguides and microcavities can be designed and optimized utilizing PC reflection phase. We have proposed a different application using reflection phase relationship between TE and TM waves, and a broadband half-wave plate is designed.[14] Here, this method is expanded to design broadband and angle-insensitive phase retarders with arbitrary phase shift difference.

A. Broadband phase retarder

A broadband half-wave plate is designed. The unit cell of the structure consists of a cross in the air background, with a square in the middle, as is shown in Fig. 5(a). The structure is a square lattice with a lattice constant of a. In each cross, the widths of each branch are dx and dz, and the width of the central square is d. The length in the z direction is L, the incident angle is θ, and the index of refraction of the dielectric material is n, shown in black color in the figure. The index of air is $n_0=1.0$. n is set as 3.4, the index of silicon for a wavelength of 1.55 μm. For application, θ is set as 45°, and $L=8a$ for high reflection. By varying dx, dz, and d, an optimized broadband half-wave plate is obtained. The optimized parameters are $dx=0.05a$, $dz=0.15a$, and $d=0.40a$. Figure 5(b) shows the dependence of reflectance on normalized frequency. In the common reflection region, $\omega a/2\pi c = (0.2528-0.3408)$, with reflectance more than 99.9%. Figure 5(c) shows the dependences of reflection phase shift Φ_{TE} (solid line), Φ_{TM} (dotted line) and reflection phase shift difference $\Delta\Phi=\Phi_{TM}-\Phi_{TE}$ (dashed-dotted line) on frequency. A half-wave plate can be obtained for $\Delta\Phi=\pi$. Set tolerance $=0.01\pi$ (the accuracy of the usual wave plate), where PC can be regarded as a half-wave plate for $|\Delta\Phi-\pi| \leq$ tolerance. This tolerance requirement can be met in the frequency range $\omega a/2\pi c=(0.282-0.3242)$ [shown as shaded areas in Figs. 5(b) and 5(c)], where the bandwidth relative to central frequency is $\Delta\omega/\omega \approx 13.7\%$.

By only varying the structural parameters and thus the relative position of the stop bands of two polarizations, quarter-wave plate can also be obtained. The proposed structure is same as that in Fig. 5(a), with different structural parameters. The optimized parameters are $dx=dz=0.06a$, with the width of the square of $d=0.42a$. Other parameters are same as $\theta=45°$, $n=3.4$, and $L=8a$. Figure 5(d) shows the dependence of reflectance on normalized frequency. Figure 5(e) shows the dependences of reflection phase shift Φ_{TE} (solid line), Φ_{TM} (dotted line), and reflection phase shift difference $\Delta\Phi=\Phi_{TM}-\Phi_{TE}$ (dashed-dotted line) on frequency. For quarter-wave plate, it is required that $|\Delta\Phi-3\pi/2| \leq$ tolerance, where tolerance$=0.01\pi$. This requirement can be met in the normalized frequency range $\omega a/2\pi c = (0.476-0.5085)$ [shown as shaded areas in Figs. 5(d) and 5(e)]. In this range, the reflectance of the two polarizations is over 99.9%, and the bandwidth relative to the central frequency is $\Delta\omega/\omega \approx 6.6\%$.

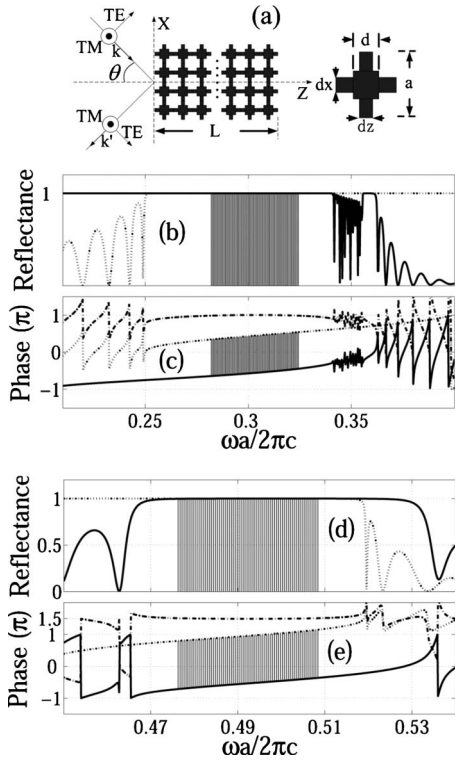

FIG. 5. (a) shows the structure of PC with square lattice and the direction regulation of electric field. $n=3.4$, $L=8a$, and $\theta=45°$. In (b), (c), (d), and (e), the solid line denotes TM wave, dotted line denotes TE wave, and dashed-dotted line denotes $\Delta\Phi=\Phi_{TE}-\Phi_{TM}$. For $dx=0.05a$, $dz=0.15a$, and $d=0.40a$, the reflectance (b) and reflection phase shift (c) vary with frequency, and the PC can be regarded as a half-wave plate in the shaded area. For $dx=dz=0.06a$ and $d=0.42a$, the reflectance (d) and reflection phase shift (e) vary with frequency, and the PC can be regarded as a quarter-wave plate in the shaded area.

In optical communication dense wavelength division multiplexing system, the relative bandwidth of the wavelength region with a central wavelength of 1.55 μm is about 6.3% (1.520 25–1.617 88 μm). The wave plates we proposed have broad enough bandwidth, and the thickness of the wave plates is no more than five times the wavelength. Therefore, in the communication wavelength range, the thickness of these wave plates is no more than 10 μm. Moreover, 2D PCs are easy to integrate with other optical components using highly developed semiconductor technology.

Using the unique properties of reflection phase of TE and TM wave within the stop band and their relationship, broad bandwidth phase retarder (wave plate is one of its special type) with arbitrary phase difference can be designed in principle. Meanwhile, unlike traditional wave plates that utilize anisotropic crystal to retard phase, we achieve an an-

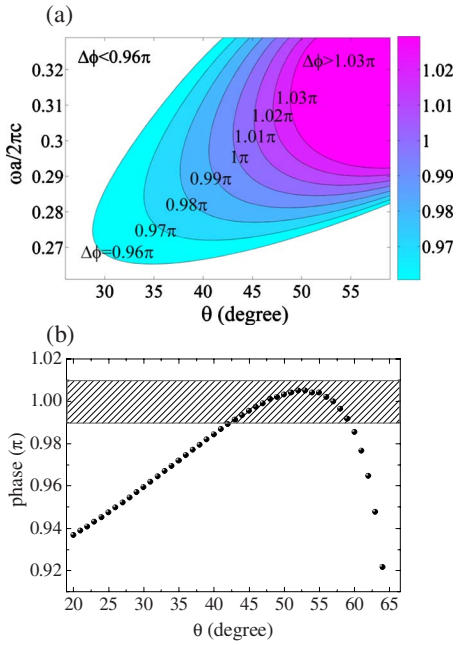

FIG. 6. (Color online) (a) shows the contour of phase difference $\Delta\Phi$ as a function of normalized frequency and incident angle. (b) shows the dependence of $\Delta\Phi$ on incident angle with fixed normalized frequency of 0.285. The structure parameters are same with those of Figs. 5(b) and 5(c). $dx=0.05a$, $dz=0.15a$, and $d=0.40a$.

isotropic control of light by adjusting the structure without constraining on the material itself. Our method will provide a flexible choice for the fabrication of a variety of broadband phase retarder used in optoelectronic integration.

B. Angle-insensitive phase retarder

Phase retarder usually presents angle dependence. An angle-insensitive phase retarder is very convenient for using. For the variation behavior of phase shift in stop band is not sensitive to incident angle generally, the phase retarders designed above can remain angle-insensitive. As an example, we discuss half-wave plate shown in Figs. 5(b) and 5(c) in detail. The contour of phase difference $\Delta\Phi$ as a function of normalized frequency and incident angle has presented in Fig. 6(a). The whole displayed domain of Fig. 6(a) is almost within stop band of PC for two polarizations. As observed from Fig. 6(a), $\Delta\Phi$ varies gently in whole domain. Therefore, if the incident angle is fixed, a broad band phase retarder can be achieved; if the normalized frequency is fixed, an angle-insensitive phase retarder can be achieved. Here, as the normalized frequency is fixed as 0.285, $\Delta\Phi$ as a function of incident angle θ is shown in Fig. 6(b). With θ varying from 42° to 59°, $|\Delta\Phi-\pi| \leq$ tolerance, shown as shadow, i.e., the half-wave plate is angle-insensitive within angle region of 42° to 59°. $\Delta\Phi$ of other frequencies have alike properties.

We should mention that the 2D PC with common stop band for TE and TM waves in a certain incident direction could be a candidate for designing broadband and angle-insensitive phase retarder. The PC with full band gap would be a better one, since it can always permit common stop band for TE and TM waves for any incident direction.

VIII. CONCLUSIONS

In summary, using TMM, the properties of reflection phase shift in the stop band have been investigated. In the first stop band of PC, when high index material is distributed near the center of unit cell, the reflection phase shift in the incident TM wave approximates to $-\pi$ in the lower band edge, while it approximates to zero in the upper band edge. When low index material is near the center of the unit cell, the reflection phase shift in the incident TM wave approximates to zero in the lower band edge, while it approximates to π in the upper band edge. In most cases, the phase shift in higher-order stop band differs from that of the first stop band. The rule determining the difference is that, to a structure, there exists a certain value of filling fraction of dielectric to air. The structure with that value has a phase shift difference close to zero, while the one with a filling fraction far from that value has a significant phase shift difference. A 1D model is used as an analog to explain this interesting phenomenon. For the relationship of TE and TM wave, with proper structural parameters, the reflection phase difference between them can remain invariant in a very broad frequency range. Based on this property, we have designed broadband and angle-insensitive phase retarders, and a lot of potential applications will be brought.

ACKNOWLEDGMENTS

The authors acknowledge the financial support from the National Natural Science Foundation of China (Grant Nos. 60908040 and 10974060), the Ph.D. Programs Foundation of Ministry of Education of China (Grant No. 20094407120011), and the Natural Science Foundation of Guangdong province of China (Grant No. 9451063101002256).

[1] E. Yablonovitch, Phys. Rev. Lett. **58**, 2059 (1987).
[2] S. John, Phys. Rev. Lett. **58**, 2486 (1987).
[3] L.-M. Li, Appl. Phys. Lett. **78**, 3400 (2001).
[4] D. R. Solli, C. F. McCormick, and R. Y. Chiao, Appl. Phys. Lett. **82**, 1036 (2003).
[5] D. R. Solli, C. F. McCormick, R. Y. Chiao, and J. M. Hickmann, J. Appl. Phys. **93**, 9429 (2003).
[6] F. Miyamaru, T. Kondo, T. Nagashima, and M. Hangyo, Appl. Phys. Lett. **82**, 2568 (2003).
[7] M. Iwanaga, Appl. Phys. Lett. **92**, 153102 (2008).
[8] W. F. Zhang, J. H. Liu, W.-P. Huang, and W. Zhao, Opt. Lett. **34**, 2676 (2009).
[9] S. Noda, M. Yokoyama, M. Imada, A. Chutinan, and M. Mochizuki, Science **293**, 1123 (2001).
[10] L. Frandsen, P. Borel, Y. Zhuang, A. Harpøth, M. Thorhauge, M. Kristensen, W. Bogaerts, P. Dumon, R. Baets, V. Wiaux, J. Wouters, and S. Beckx, Opt. Lett. **29**, 1623 (2004).
[11] Z. Wang and S. Fan, Opt. Lett. **30**, 1989 (2005).
[12] E. Istrate and E. H. Sargent, Appl. Phys. Lett. **86**, 151112 (2005).
[13] E. Istrate, A. A. Green, and E. H. Sargent, Phys. Rev. B **71**, 195122 (2005).
[14] Q. F. Dai, Y. W. Li, and H. Z. Wang, Appl. Phys. Lett. **89**, 061121 (2006).
[15] R. M. Bell, J. B. Pendry, L. Martin Moreno, and A. J. Ward, Comput. Phys. Commun. **85**, 306 (1995).
[16] S. G. Johnson and J. D. Joannopoulos, Opt. Express **8**, 173 (2001).
[17] J. D. Joannopoulos, R. D. Meade, and J. N. Winn, *Photonic Crystals: Molding the Flow of Light* (Princeton University Press, Princeton, NJ, 1995).
[18] R.-L. Chern and S. D. Chao, Opt. Express **16**, 16600 (2008).